

Nickel Coatings Electrodeposited from Watts Type Baths Containing Quaternary Ammonium Sulphate Salts

Jarosław Wojciechowski¹, Marek Baraniak¹, Juliusz Pernak², Grzegorz Lota^{1,*}

¹ Poznan University of Technology, Institute of Chemistry and Technical Electrochemistry, Berdychowo 4, 60-965 Poznan, Poland

² Poznan University of Technology, Institute of Chemical Technology and Engineering, Berdychowo 4, 60-965 Poznan, Poland

*E-mail: grzegorz.lota@put.poznan.pl

Received: 5 January 2017 / Accepted: 23 February 2017 / Published: 12 March 2017

The paper presents the anti-corrosive properties of nickel coatings, deposited on the surface of the steel AISI 1018 from Watts type baths, containing protic and aprotic quaternary ammonium sulphate salts additives. Nickel electrodeposition was carried out using two different values of current density. Four different solutions contained protic and aprotic quaternary ammonium sulphate salts with a different number of carbon atoms in the alkyl chain. Scanning electron microscope and X-ray scattering methods were used to analyse the surface of obtained coatings. Anti-corrosive properties were determined by means of electrochemical impedance spectroscopy measurements. The results demonstrate a significant effect of current density values on the texture and thickness of the nickel coatings, and quaternary ammonium salts on their anti-corrosive properties. Samples containing aprotic salts with three -CH₃ substituents and the carbon chain of 6 carbon atoms inhibit the corrosion process to the greatest extent.

Keywords: Corrosion protection, Electrochemical impedance spectroscopy, Nickel coating, Quaternary ammonium salt

1. INTRODUCTION

Electrodeposition of nickel has been investigated intensely during the last few decades to enable the efficient production of various details and elements. Electroplated coatings of nickel are commercially very important and up to 150 000 tonnes are annually deposited worldwide [1-3]. Nickel layers are prepared for many reasons. Nickel provides a decorative appearance because of its ability to cover defects of the base metal. This deposit can be made brilliant especially when it is covered

additionally by a thin layer of decorative chrome. The nickel coatings also show corrosion protective features. Corrosion protection can be increased, for example, by combining two kinds of nickel plating (semi-bright and bright nickel) or by nickel layer, modified to increase its hydrophobic properties [1,3,4]. Nickel coating is also preferable, when higher wear resistance is necessary compared to zinc or copper. The nickel layer has a low coefficient of friction. Additionally, nickel has ferromagnetic properties and steel may be deposited by nickel without changing its magnetic properties [1-3]. The nickel electrodeposition process may be conducted using a few different types of aqueous baths [1,3-5]. In addition, others aqueous solutions, deep eutectic solvents or even molten salt are still under research [5-7]. The cathode current efficiency of different nickel electroplating solutions is usually above 90%. The lower efficiency is observed for some bright nickel solutions which have been formulated to provide a high level of brilliance. Values over 95% are usually achieved on additive-free nickel solutions. The important problems of nickel electrodeposition include: adhesion or even peeling off, and pitting on layer [1,3,8-11]. The most popular baths, among industrial methods of electrodeposition of nickel are Watts-type solutions. This type of bath was invented about 100 years ago by O.P. Watts. Basic compounds in this type of bath are nickel sulphate, nickel chloride and boric acid. These baths may contain many types of organic additives [1,3,5,8,11-16]. These compounds are usually divided into two groups/types. Type I serves as a carrier and reducer of the stresses occurring in the coating crystalline layer in the nickel electroplating bath. Internal stress refers to forces created in the layer as a result of the electrocrystallization process on another material and sometimes as a result of co-deposition of heteroatoms. This type of additive has usually an aromatic structure with sulphur, for example: benzene sulphonic acid, 1,3,6-naphthalene sulphonic acid (sodium salt), p-toluene sulphonamide, saccharin and allylsulphonic acid. Carriers introduce sulphur into the deposit. Type II additives are commonly known as brighteners. Today a wide range of organic compounds are used. They include: formaldehyde chloral hydrate, o-sulphobenzaldehyde, allylsulphonic acid, 2-butyne-1, 4-diol, thiourea, coumarin and many others. Brighteners are generally present in very low concentrations and are consumed by electrolysis. This generates problems with suitable additives determination in bath [17].

In this paper, we present the influence of selected protic and aprotic quaternary ammonium sulphate salt additives in the Watts type bath on anti-corrosive properties of electrodeposited nickel coatings. Electrochemical as well as surface analysis techniques were applied to characterize anti-corrosive properties and surface morphology of obtained samples.

2. EXPERIMENTAL

2.1. Electrodeposition of nickel coatings.

At first, steel AISI 1018 discs (Rowitex Company) with the diameter of 30 mm were pre-treated i.e. cleaned mechanically using abrasive paper with granulation 2500, degreased in a solution containing 15 g dm^{-3} NaOH and 30 g dm^{-3} $\text{Na}_3\text{PO}_4 \cdot \text{H}_2\text{O}$ (298 K, 10 minutes) and etched in a solution of 1M HCl (298 K, 5 min). Between each of these stages, the steel surface was rinsed with distilled

water. Thus prepared samples were then subjected to a nickel electrodeposition process from four different Watts type baths, containing: $250 \text{ g dm}^{-3} \text{ NiSO}_4 \cdot 7\text{H}_2\text{O}$, $30 \text{ g dm}^{-3} \text{ NiCl}_2 \cdot 6\text{H}_2\text{O}$ and $40 \text{ g dm}^{-3} \text{ H}_3\text{BO}_3$ (pH 4.3-4.4). Additionally, each of these four baths contains protic or aprotic quaternary ammonium sulphate salt additives (QAS) (500 mg dm^{-3}), with a various number of carbon atoms prevalent in the alkyl chain. The process of nickel electrodeposition was performed on the steel cathode surface using two different current density values: (A) 100 mA dm^{-2} , and (B) 350 mA dm^{-2} . Table 1 shows the signature of all prepared samples. All chemical reagents were purchased from Sigma Aldrich. Quaternary ammonium salts were synthesised in the Institute of Chemical Technology and Engineering at Poznan University of Technology.

Table 1. Signature of samples with nickel coatings deposited from four different Watts type baths using two different current density values.

Sample	Current density/ mA dm^{-2}	Quaternary ammonium sulphate
AC6H	(A) 100	Protic, $-\text{CH}_3$, $-\text{CH}_3$, $\text{R}=\text{C}_6$
AC16H	(A) 100	Protic, $-\text{CH}_3$, $-\text{CH}_3$, $\text{R}=\text{C}_{16}$
AC6	(A) 100	Aprotic, $-\text{CH}_3$, $-\text{CH}_3$, $-\text{CH}_3$, $\text{R}=\text{C}_6$
AC16	(A) 100	Aprotic, $-\text{CH}_3$, $-\text{CH}_3$, $-\text{CH}_3$, $\text{R}=\text{C}_{16}$
BC6H	(B) 350	Protic, $-\text{CH}_3$, $-\text{CH}_3$, $\text{R}=\text{C}_6$
BC16H	(B) 350	Protic, $-\text{CH}_3$, $-\text{CH}_3$, $\text{R}=\text{C}_{16}$
BC6	(B) 350	Aprotic, $-\text{CH}_3$, $-\text{CH}_3$, $-\text{CH}_3$, $\text{R}=\text{C}_6$
BC16	(B) 350	Aprotic, $-\text{CH}_3$, $-\text{CH}_3$, $-\text{CH}_3$, $\text{R}=\text{C}_{16}$

2.2. Surface morphology analysis.

Scanning electron microscope (SEM EVO[®] 40 ZEISS) was used to characterise surfaces of steel AISI 1018 with electrodeposited nickel coatings. Additionally, the wide angle X-ray scattering (XRD) method with CuK α radiation wavelength of 1.5418 \AA (Philips, PW 1050) was used to examine the structure and crystallinity of the electrodeposited nickel. The X-ray diffraction patterns were recorded at an angle (2θ) range of $10\text{-}70^\circ$, with a scan step of 0.04° .

2.3. Electrochemical measurements.

Electrochemical measurements were performed in a Plexiglas[®] three-electrode cell systems. Saturated calomel electrodes (SCE) and platinum plates served as a reference and counter electrodes, respectively. Nickel electrodeposited plates were used as working electrodes. All the electrochemical tests were made in a 3.5% NaCl solution (Sigma Aldrich) at ambient conditions, using an electrochemical workstation potentiostat/galvanostat VMP3 (Biologic, France) with impedance module.

In the beginning, the open circuit potential (ocp) of samples was measured for 240 minutes. After that, electrochemical impedance spectroscopy (EIS) tests were performed in the frequency range from 100 kHz to 10 mHz. The amplitude of the applied signal was ± 10 mV versus open circuit potential.

3. RESULTS AND DISCUSSION

3.1. Surface morphology analysis.

Fig. 1(a-d) show the SEM images of samples AC6H, BC6H, AC16 and BC16. As has been mentioned, samples AC6H and AC16 contain nickel coatings, deposited on the steel surface using a current density of 100 mA dm^{-2} , while samples BC6H and BC16 using 350 mA dm^{-2} . On the basis of Fig. 1, it can be seen that the type of QAS addition does not in any way affect the appearance of the resulting coating of nickel. An important aspect for the coating grains size is the value of the current density. With a constant concentration of the organic additive (QAS) and increased current density, nickel coatings with larger grains are formed (Fig. 1(b, d)) [10,18].

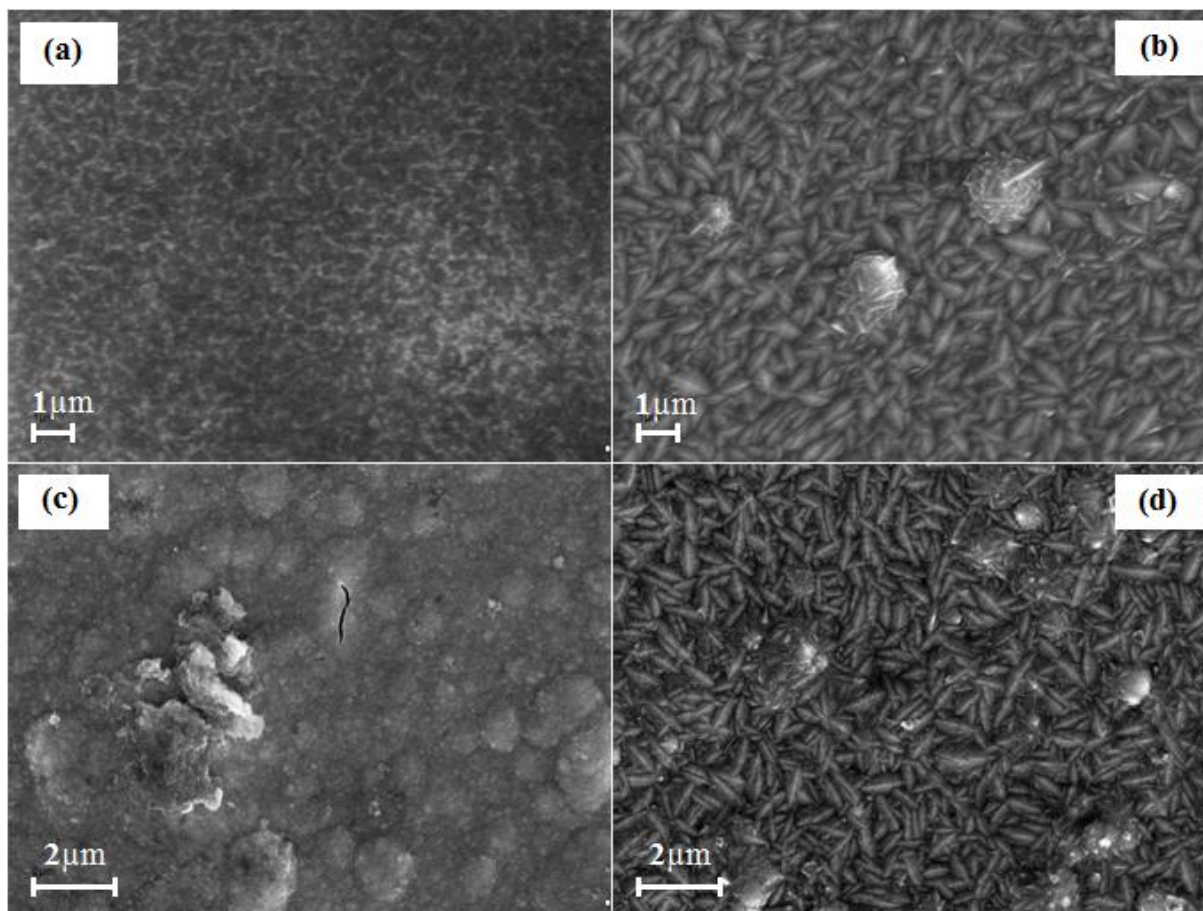


Figure 1. Scanning electron microscope (SEM EVO[®] 40 ZEISS) images of samples: (a) AC6H, (b) BC6H, (c) AC16, (d) BC16.

Rashidi and Amadeh [10] found that increasing the current density to 200 mA dm^{-2} it is possible to obtain nickel coatings with smaller grains. In contrast, values higher than 200 mA dm^{-2} formed coatings with a larger grain structure. Most likely, a high current density causes a loss of nickel ions in the space near the cathode. In addition, hydrogen evolves on the electrode. Thus, the current is then compensated by the two competing reactions i.e. reduction reactions of nickel and hydrogen. In this case, the current density of 100 mA dm^{-2} forced the formation of thinner nickel coatings, characterized by finer grains (Fig. 1(a, c)) in comparison to coatings created using a current density of 350 mA dm^{-2} (Fig. 1(b, d)) [10,18].

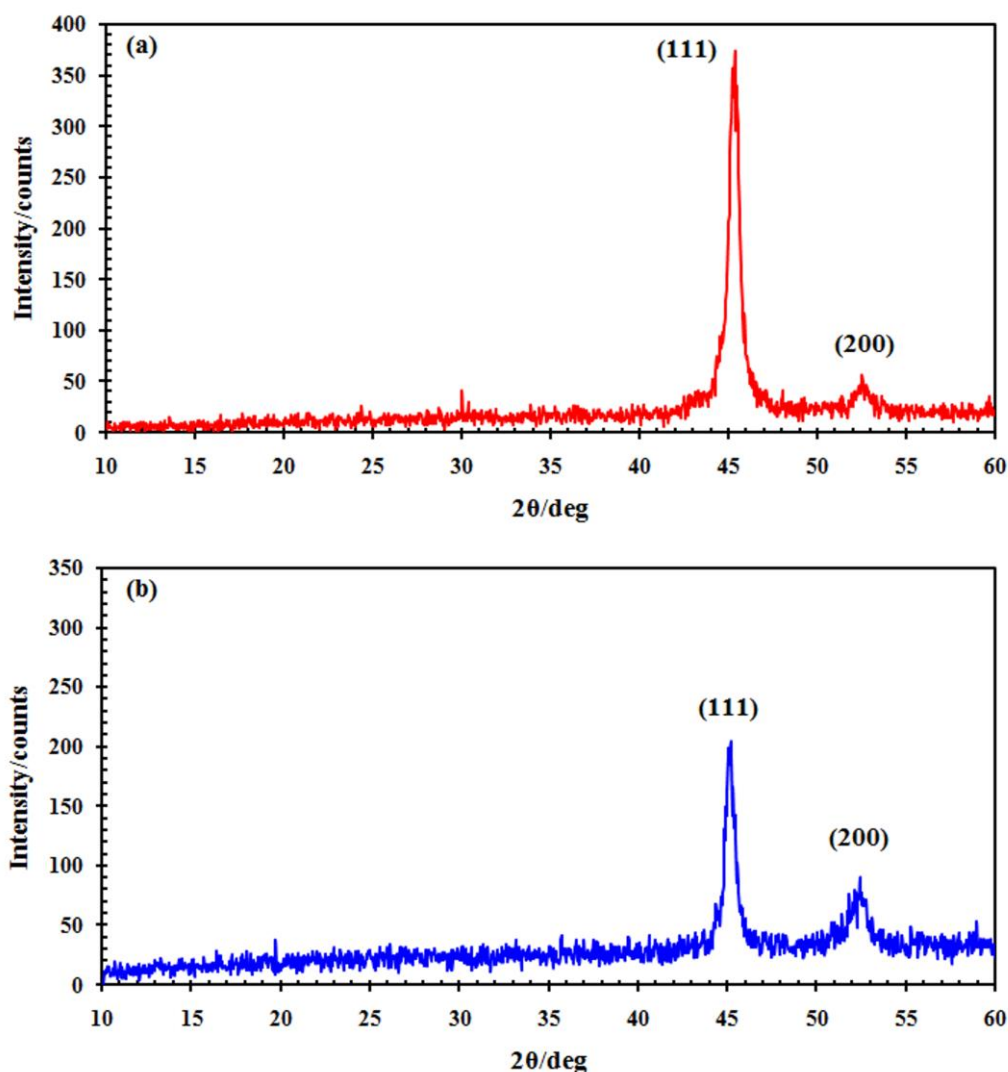


Figure 2. The X-ray diffraction patterns of samples: (a) AC6H and (b) BC6H.

Fig. 2(a-b) present X-ray diffraction patterns of samples with nickel coatings deposited using two different values of current density i.e. 100 mA dm^{-2} (AC6H) and 350 mA dm^{-2} (BC6H). Those results confirm assumptions based on SEM characterization. Crystals of both coatings tend to grow in two directions of (111) and (200) planes. However, depending on the value of applied current density,

the ratio between two planes is significantly different. Concentration of the QAS additive used in Watts type bath was constant. Thus, the only influence on crystals orientation is caused by applied current density. Ratio (200)/(111) is lower for coatings with finer grains [10,18].

3.2. Electrochemical measurements

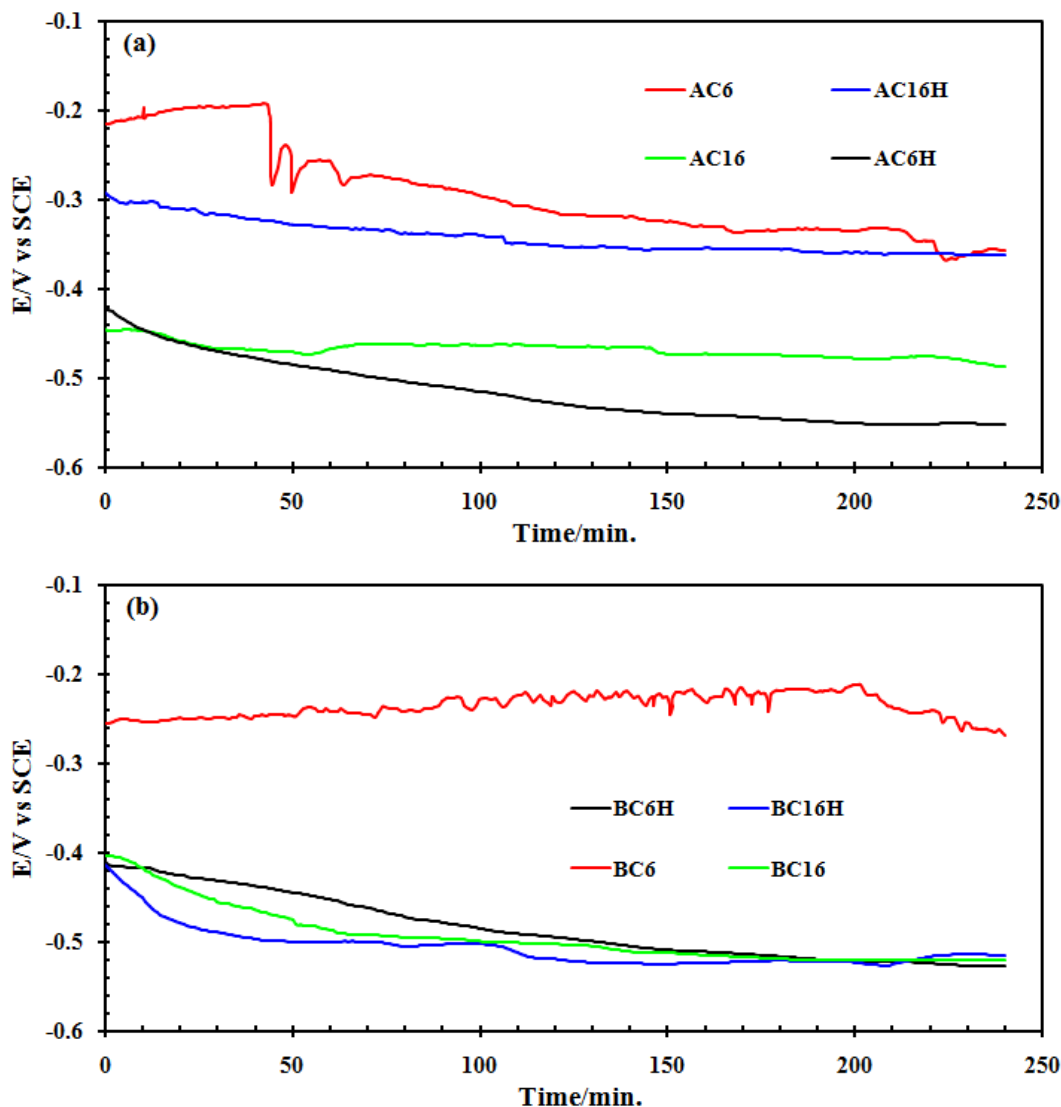


Figure 3. Open circuit potential measurements of the samples with nickel coatings, electrodeposited using two different current density values: (a) 100 mA dm^{-2} and (b) 350 mA dm^{-2} .

Fig. 3(a-b) show the curves of potential measurements at open circuit conditions for all received samples. On the basis of these results it is concluded that the corrosion process i.e. dissolution reaction of the nickel is the slowest in the case of samples AC6 and BC6, which contain coatings, deposited from baths with aprotic QAS additive, containing 6 carbon atoms substituent. The values of the potentials of these samples were the highest (most noble), i.e. the corrosion process proceed slowly on the surface of nickel coating.

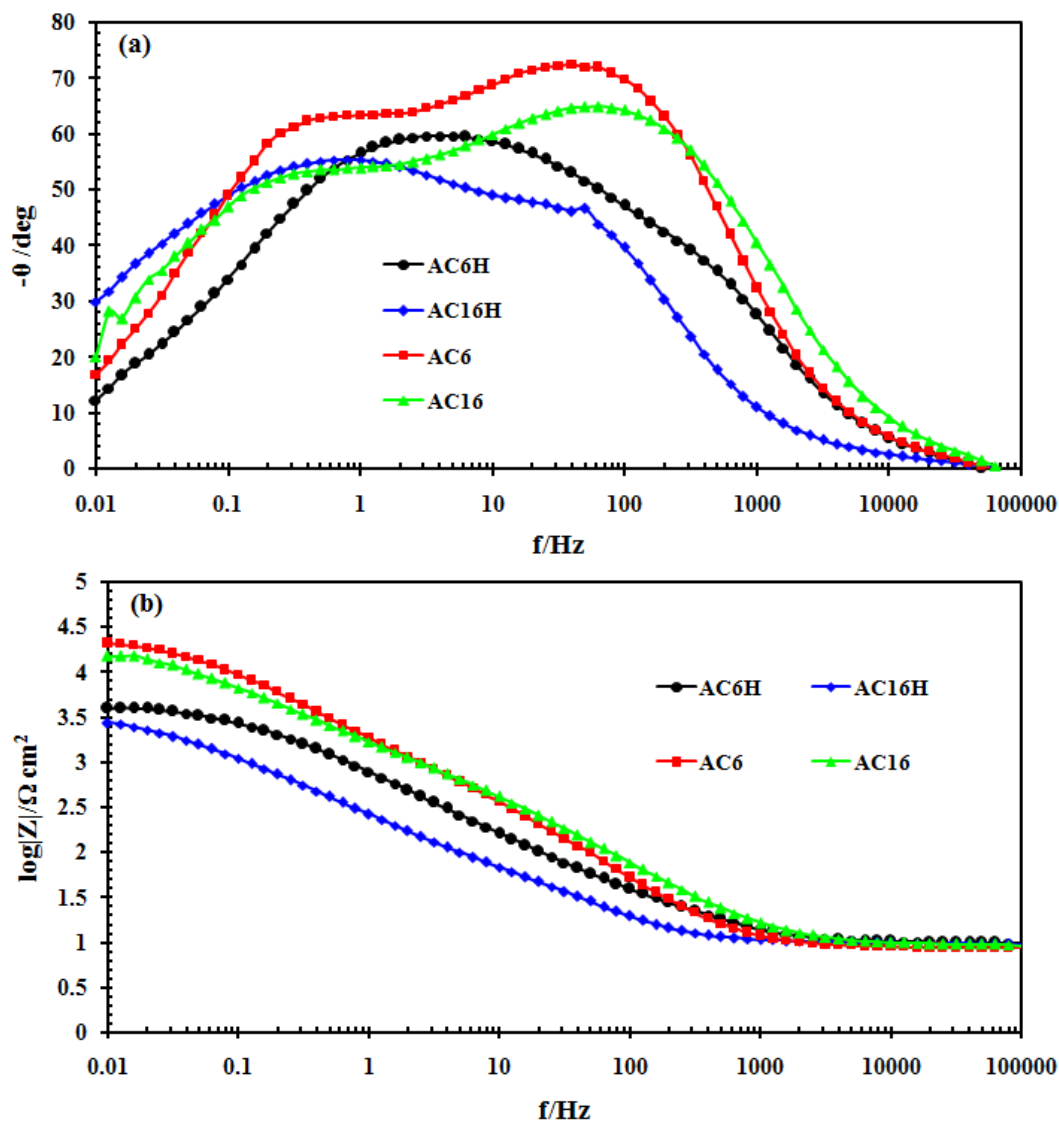


Figure 4. Bode plots of the samples with nickel coatings, electrodeposited using current density 100 mA dm^{-2} : (a) phase angle and (b) impedance modulus.

Fig. 4(a-b) show Bode plots for the samples coated with nickel, deposited using a current density of 100 mA dm^{-2} . In the case of the phase angle values, depending on the frequency, each of the curves show two time constants which are visible in two indistinct and poorly separated loops. As has been mentioned previously, on the basis of the SEM images, the coating deposited using a current density of 100 mA dm^{-2} are thinner, and characterized by a finer grain structure [10,18]. As a result, in Fig. 4(a), there are two time constants. The first loop that appears in the higher frequency range illustrates the behaviour of the nickel coating, deposited on the surface of the steel AISI 1018. The second loop, prevalent in the lower range of frequencies refers to the formation of the electrical double layer at the steel/nickel interface. Both loops are poorly separated. The values of the phase angle between them do not reach -45° . In the high frequency range, phase angle is close to zero. Only by decreasing the frequency, applied signal is able to penetrate the nickel coating. Thus the sample begins to behave like a capacitor, despite the fact that nickel as the metal is a very good conductor [19]. This

is most likely due to the presence in its structure of QAS additive molecules, comprising carbon chains.

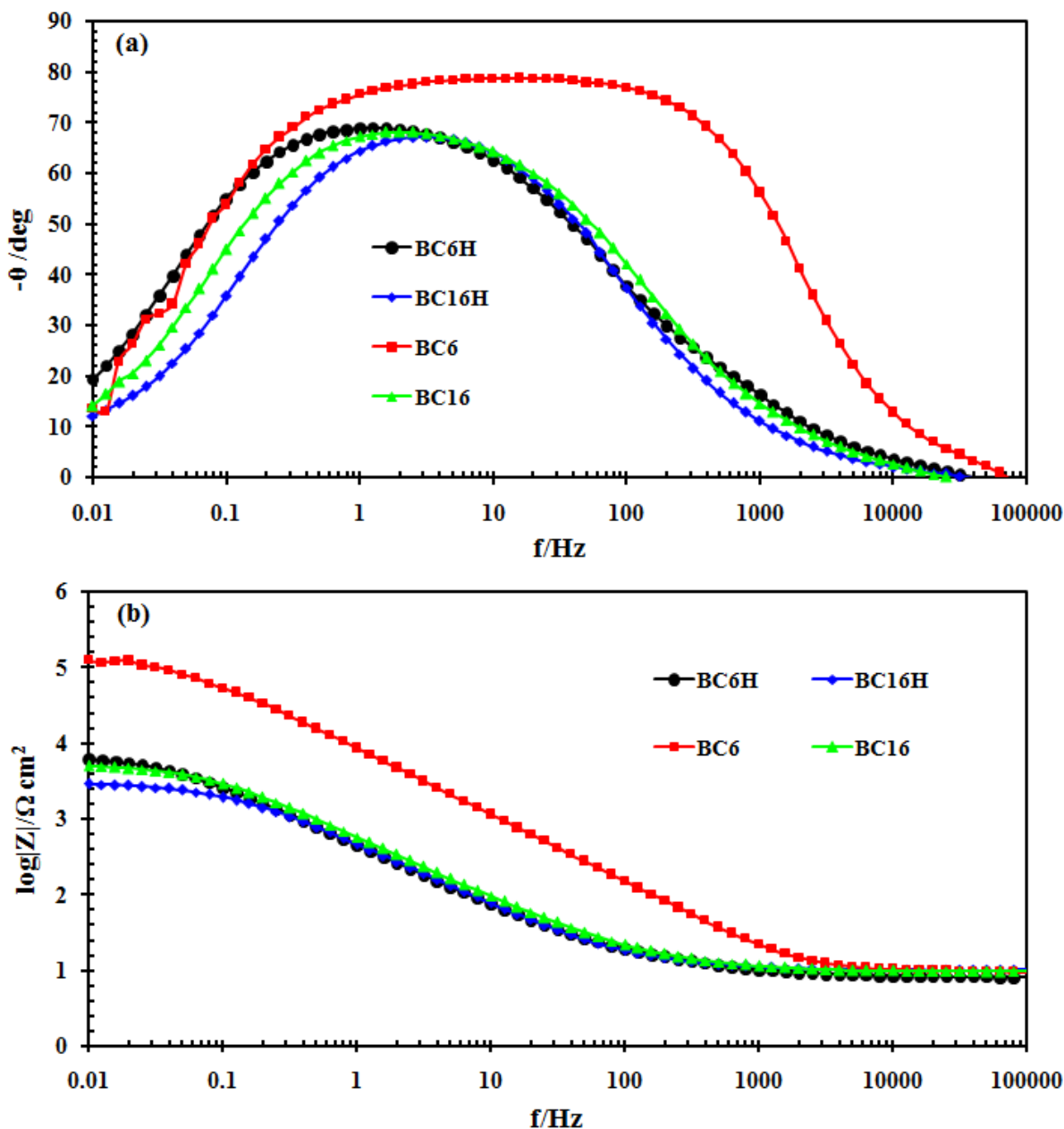


Figure 5. Bode plots of the samples with nickel coatings, electrodeposited using current density 350 mA dm^{-2} : (a) phase angle and (b) impedance modulus.

Fig. 4(b) shows the relationship between impedance modulus and frequency of the applied signal. In this case the curves also show two time constants relating to the nickel coating and steel surface. In the high frequency range, there is a plateau, then the slope of curves is equal to -1, which indicates that the samples start to behave like a capacitor. In the frequency range between 100 Hz and 1 Hz shape of the curves is changing. This is due to the appearance of the second time constant

resulting from the formation of the electrical double layer at the steel/nickel interface. In the low frequency range there is a plateau which indicates electrode reactions at the steel/nickel interface. The electrical equivalent circuit element representing electrode reactions is a resistor [19].

Fig. 5(a-b) show Bode plot for the steel samples, coated with nickel using a current density of 350 mA dm^{-2} . As has been already mentioned, coatings of the samples BC6H, BC16H, BC6, and BC16 are characterized by a much larger grains size. The coating itself was also thicker than the coating deposited using a current density of 100 mA dm^{-2} [10,18]. As a result, this coating is responsible for the existence of one time constant (one loop) on the Bode plots (Fig. 5(a)). In this case applied signal does not penetrate the steel/nickel interface in the considered frequency range. Fig. 5(b) presents the curves with a slope of -1 and two plateau regions at high and low frequencies that correspond to an equivalent series resistance, attributed to a electrolyte and nickel coating, respectively [19]. On the basis of the obtained results, electrical equivalent circuits have been fitted to tested samples [19]. Fig. 6(a) shows an electrical equivalent circuit corresponding to coatings with finer grains (AC6H, AC16H, AC6 and AC16), which indicate two time constants. The elements of this circuit are R_s - equivalent series resistance of the electrolyte solution, C_c - capacitance of the nickel coating, R_c - resistance of the nickel coating, C_{dl} - capacitance of the electrical double layer at the steel/nickel interface, R_{ct} - resistance of the reactions at the steel/nickel interface. Fig. 6(b) shows an electrical equivalent circuit with one $C_c R_c$ time constant attributed to coatings with larger grains.

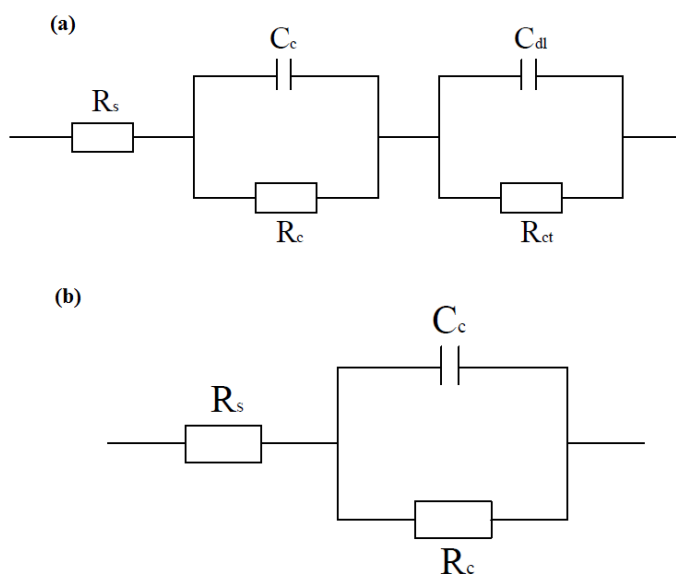


Figure 6. Equivalent circuits fitted to samples: (a) AC6H, AC16H, AC6, AC16 and (b) BC6H, BC16H, BC6, BC16.

Bode plots in Fig. 4(a-b) and 5(a-b) show the influence of the QAS additive structure on the anti-corrosive properties of the obtained nickel coatings. Samples containing coatings with protic QAS additives have worse anti-corrosive properties than their aprotic counterparts. The impedance modulus values at a frequency of 10 mHz are greater for the samples AC6, AC16, BC6, and BC16 when

compared to samples AC6H, AC16H, and BC6H, BC16H. The addition of QAS inhibits the nickel reduction reaction. Grain growth process is blocked and overpotential of metal deposition is shifted. Electropositive charge on the nitrogen atom is greater in the case of protic QAS cations than in their aprotic counterparts where there are more $-\text{CH}_3$ substituents. As a result, protic QAS more effectively stabilize the Ni^{2+} ions, contained in the Watts type bath in the form of negative borate complexes. Therefore, the settlement of aprotic QAS in nickel coating proceed faster.

Comparing the effect of alkyl chain length on the anti-corrosive properties of the obtained nickel coatings, it is concluded that the corrosion process is slower at the surface of coatings comprising QAS with 6 carbon atoms rather than 16. Probably more cations having a substituent with 6 carbon atoms are incorporated into a nickel coating, making it more hydrophobic. This is caused by steric hindrance of the ion containing 16 carbon atoms.

4. CONCLUSIONS

The nickel coatings were deposited on the surface of the steel AISI 1018 from Watts type baths, containing quaternary ammonium sulphate salts using two different current densities. A lower current density value caused the creation of thinner coatings with finer grains. The study of electrochemical impedance spectroscopy allowed differentiating two time constants, corresponding to nickel coating and the formation of the electrical double layer at the steel/nickel interface. Thicker coatings with larger grains performed only one time constant, depicting the characteristics of nickel, which in a certain frequency range behaves like a capacitor. This is due to the presence of quaternary ammonium salts in its structure. Construction of those compounds also had a significant influence on the characteristics of the obtained Bode plots. Samples containing aprotic salts with three $-\text{CH}_3$ substituents and the alkyl chain of 6 carbon atoms exhibited the best anti-corrosive properties. The adsorption process of protic salts and salts with 16 carbon atoms in the alkyl chain proceeded more slowly due to the inductive and steric effects.

ACKNOWLEDGMENTS

The authors would like to gratefully acknowledge the financial support from the Ministry of Science and Higher Education of Poland, project no. 03/31/DSPB/0337.

References

1. "Nickel Plating Handbook" Nickel Institute Brussels, Belgium 2014 access 16.12.2016, https://www.nickelinstitute.org/~media/Files/TechnicalLiterature/NPH_141015.ashx.
2. R. N. Gay, K. R. Wayne, Process for Electroplating Nickel over Stainless Steel. US Patent 4, 764, 260, 1988.
3. M. Schlesinger and M. Paunovic, Modern Electroplating (fifth ed.), John Wiley & Sons, (2010) New Jersey, USA.
4. S. Khorsand, K. Raeissi and F. Ashrafizadeh, *Appl. Surf. Sci.*, 305 (2014) 498.

5. A. P. Abbott, A. Ballantyne, R. C. Harris, J. A. Juma, K. S. Ryder and G. Forrest, *Electrochim. Acta*, 176 (2015) 718.
6. C. Li, X. Li, Z. Wang and H. Guo, *Rare Metal Mat. Eng.*, 44 (2015) 1561.
7. Q. Zhang and Y. Hua, *Chin. J. Chem. Eng.*, 21 (2015) 1397.
8. U. S. Mohanty, B. C. Tripathy, P. Singh, and S. C. Das, *J. Appl. Electrochem.*, 31 (2001) 579.
9. D. Oloruntoba, O. Eghwubare and O. Oluwole, *Leonardo El. J. Pract. Technol.*, 18 (2011) 79.
10. A. M. Rashidi and A. Amadeh, *J. Mater. Sci. Technol.*, 26 (2010) 82.
11. O. Sadiku-Agboola, E. R. Sadiku and O. F. Biotidara, *Int. J. Phys. Sci.*, 7 (2012) 349.
12. D. Mockute and G. Bernotiene, *Surf. Coat. Technol.*, 135 (2000) 42.
13. S. Wehner, A. Bund, U. Lichtenstein, W. Plieth, W. Dahms and W. Richtering, *J. Appl. Electrochem.*, 33 (2003) 457.
14. E. M. Oliveira, G. A. Finazzi and I. A. Carlos, *Surf. Coat. Technol.*, 200 (2006) 5978.
15. E. A. Pavlatou, M. Raptakis and N. Spyrellis, *Surf. Coat. Technol.*, 201 (2007) 4571.
16. Y. Nakamura, N. Kaneko, M. Watanabe and H. Nezu, *J. Appl. Electrochem.*, 24 (1994) 227.
17. M. Vidal, J. M. Amigo, R. Bro, M. Ostra and C. Ubide, *Anal. Methods*, 2 (2010) 86.
18. F. Ebrahimi and Z. Ahmed, *J. Appl. Electrochem.*, 33 (2003) 733.
19. A. Lasia, *Electrochemical Impedance Spectroscopy and its Applications*, Springer, (2014) New York, USA.